Progress In Electromagnetics Research M, Vol. 47, 129–139, 2016

Device-Free Electromagnetic Passive Localization with Frequency Diversity

Wei Ke[1, 2], Yanan Yuan[1], Xiunan Zhang[1], and Jianhua Shao[1, *]

Abstract—As an emerging wireless localization technique, the electromagnetic passive localization without the need of carrying any device, named device-free passive localization (DFPL) technique has drawn considerable research attention. The DFPL technique detects shadowed links in the monitored area and realizes localization with the received signal strength (RSS) measurements of these links. However, the current RSS-based DFPL techniques have two major challenges: one is that the RSS signal is particularly sensitive to noise, and the other is that it needs a sufficient number of nodes to provide enough RSS measurements of wireless links to guarantee good performance. To overcome these problems, in this paper we take advantage of compressive sensing (CS) theory to handle the spatial sparsity of the DFPL problem for reducing the number of nodes required by DFPL systems and exploit the frequency diversity technique to deal with the problem of the RSS sensitivity. Meanwhile, inspired by the fact that the target's movement is continuous and that the target's current location must be around the last location, we add prior information on the support region into the sparse reconstruction process for enhancing sparse reconstruction performance. The effectiveness and robustness of the proposed scheme are demonstrated by experimental results where the proposed algorithm yields substantial improvement for localization performance.

1. INTRODUCTION

Due to potential promising commercial and military application, wireless localization and tracking have gained considerable attention over the past decade. The research area can be divided into active and passive localization. While the active localization technique [1, 2] that equips the target with a wireless device such as a smartphone or a RFID tag has been widely studied, the passive localization technique, which could realize device-free localization, is still an emerging and challenging technique. In recent years, the low-cost DFPL which only utilizes RSS measurements of wireless links has become an attractive technology and shown enormous promise in applications ranging from intrusion detection to elder care [3, 4]. Compared with the existing device-free techniques such as infrared detector, video monitor and UWB radar detector, RSS-based DFPL brings several advantages over other technologies by being able to work in obstructed environments, see through smoke, darkness, and walls, while avoiding the privacy concerns raised by video cameras.

The basic principle of RSS-based DFPL is that when a target moves into the area within a wireless network, it may cause the changes of RSS by shadowing, reflecting, diffracting, or scattering. The shadowed links will be different when the target is locate at different locations, and this makes it possible to realize DFPL based on the link measurements [3–9]. Different from that the line-of-sight (LOS) path is dominant in an open outdoor environment, multipath is common in an indoor environment, and

Received 25 October 2015, Accepted 24 December 2015, Scheduled 2 April 2016

* Corresponding author: Jianhua Shao (shaojianhua@njnu.edu.cn).

[1] Jiangsu Key Laboratory on Optoelectronic Technology, School of Physics and Technology, Nanjing Normal University, Nanjing 210023, China. [2] Jiangsu Center for Collaborative Innovation, Geographical Information Resource Development and Application, Nanjing 210023, China.

thus the change in RSS due to target presence becomes unpredictable. In addition, the current DFPL techniques require that there should be the large number of nodes to provide sufficient wireless links, and otherwise DFPL techniques sometimes cannot achieve reasonable performance. However, in many DFPL applications, only a modest or even small set of nodes can be used due to space restriction or the requirement of rapid deploy. In this paper, we try to solve the above problem from two aspects. First, we take advantage of the sparse nature of location finding in the spatial domain to realize DFPL for reducing the number of nodes required by DFPL systems. Second, motivated by the fact that most of the commercial transceivers have the ability to change the frequency, we propose to utilize frequency diversity scheme to combine the data collected on multiple frequencies for overcoming the problem of the RSS sensitivity.

The remainder of the paper is organized as follows. Section 2 presents the related works. Section 3 analyzes the feasibility of frequency diversity in DFPL, and then describes the system model and problem formulation. In Section 4, we propose a novel CS reconstruction method by utilizing the prior information on the support region to improve reconstruction performance. Experimental results are given in Section 5. Finally, Section 6 concludes the paper.

2. RELATED WORKS

In this section, we summarize the most relevant research on DFPL. The early exploration of DFPL was performed independently and almost synchronously by Youssef et al. [4, 5] and Zhang et al. [6, 7]. Zhang et al. [6, 7] presented a geometric method, and adopted the dynamic cluster-based algorithm to solve the DFPL problem. They also proposed a real-time and scalable system for realizing DFPL, where they divided the tracking field into areas and used the support vector regression model to locate the target in each area. These works proved the feasibility of utilizing wireless link information to realize DFPL. In parallel, references [4, 5] modeled the DFPL problem as a machine learning problem and realized DFPL with a fingerprint-matching method. As the fingerprinting method used in the device-dependent localization system, this method need build an offline radio map by placing the target at every possible location and store the wireless link measurements. However, the training measurements increase exponentially with the increase of the number of wireless links and targets. In addition, this method is also environment dependent and any significant change on the topology implies a costly new recalibration. Another approach to RSS-based DFPL named radio tomographic imaging (RTI) [8, 9], estimates the changes in the radio frequency (RF) propagation field of the monitored area and then forms an image of the changed field. This image is then used to infer the locations of targets within the deployed network. The drawback of RTI-based systems is that information can be lost in the two-step process [9]. Moreover, the sufficient number of nodes is required to achieve high-accuracy imaging results, such as 28 nodes in [8] and 30 nodes in [9].

Due to its excellent performance in sparse reconstruction, CS has been widely applied to realize wireless localization problem. However, most CS-based localization researches concentrated on device-dependent methods, and few works adopted the CS method to realize DFPL [10–12]. To the best of our knowledge, Kanso and Rabbat carried out the first sparsity-based work to combine RF tomography and CS to solve the DFPL problem [10]. They used the l_1 norm minimization scheme to estimate the location of the target and achieved better performance than the regularization method. In [11, 12], the greedy algorithms were used to estimate targets' positions in DFPL systems, which results in a substantial reduction of the amount of measurements. The reference [13] exploited the dictionary learning technique to adjust the basis matrix in order to compensate the inaccuracy of the basis matrix.

Despite having made a mighty advance in DFPL, deriving a target's location by exploiting RSS changes is still a challenging problem. One vital challenge for the RSS-based DFPL comes from the noise sensitive nature of the RSS, and a slight variation of the environment will cause the variations of RSS measurements. Moreover, many experiments have demonstrated that in the cluttered indoor environment, a number of factors affect the RF signal propagation including multi-path, channel fading, temperature and humidity variations, etc. Therefore, in many DFPL applications the presence of people is not the only factor affecting the propagation of radio signals. On the other hand, most DFPL methods require the sufficient number of nodes to provide enough wireless links traveling through the deployment area. But these methods are inefficient and sometimes even infeasible, since in many situations only a

modest set of wireless nodes is available.

To overcome the above limitation, we propose a new scheme to combine the frequency diversity technique and CS theory into a unified DFPL system. This novel method can make use of link information of multiple channels simultaneously to reduce the impact of the RSS sensitivity based on the fact that the influence of the noise for different channels is also different. Moreover, with link measurement information increased, the localization performance of DFPL can also be improved without increasing the number of nodes in the wireless networks.

3. PROBLEM FORMULATION

In this section, we first analyzes the feasibility of frequency diversity in DFPL, and then describes the system model and problem formulation under the multi-frequency (MF) condition.

3.1. Feasibility of the MF-DFPL System

Nowadays, most DFPL systems make use of the low-power IEEE 802.15.4-compliant radio devices in the 2.4 GHz band. The IEEE 802.15.4 standard specifies 16 channels within the 2.4 GHz band. They are numbered from 11 through 26 and are 5 MHz apart, having a 2 MHz bandwidth. This provides the technical basis to use RSS measurements from multiple channels to enhance the localization accuracy.

To verify the feasibility of the proposed scheme, an example multi-channel RSS measurement is shown in Figs. 1(a) and (b). From Fig. 1(a), we can obviously find that the architecture of the MF-DFPL is nearly the same as that of the traditional single-frequency (SF) DFPL, except that the wireless links are made up of links working in different frequencies. The detailed protocol for realizing MF-DFPL will be presented in the Section 5. In the experiment the wireless link from nodes 5 to 15 was selected as the testing link and a human moved in between the transmitter and receiver at sample $n = 65$ and then stood on the location (1.5 m, 3.0 m) statically. Thus, we tested the link measurements with and without a person (target), respectively. The variations of the RSS measurements on three different frequency channels at the 2.4 GHz band are shown in Fig. 1(b). From Fig. 1(b), we can find that the RSS measurements vary considerably on the different channels. On the channel with highest average RSS (#17), the person's effect is to reduce the RSS; while on the channel #23, the effect is to increase the RSS. In particular, the mean of the RSS on the channel #11 varies very small but the variance of the RSS significantly varies on channel #11. This phenomenon shows that the influence of the noise for different channels is also different. Motivated by this fact, Kaltiokallio et al. [14] proposed two

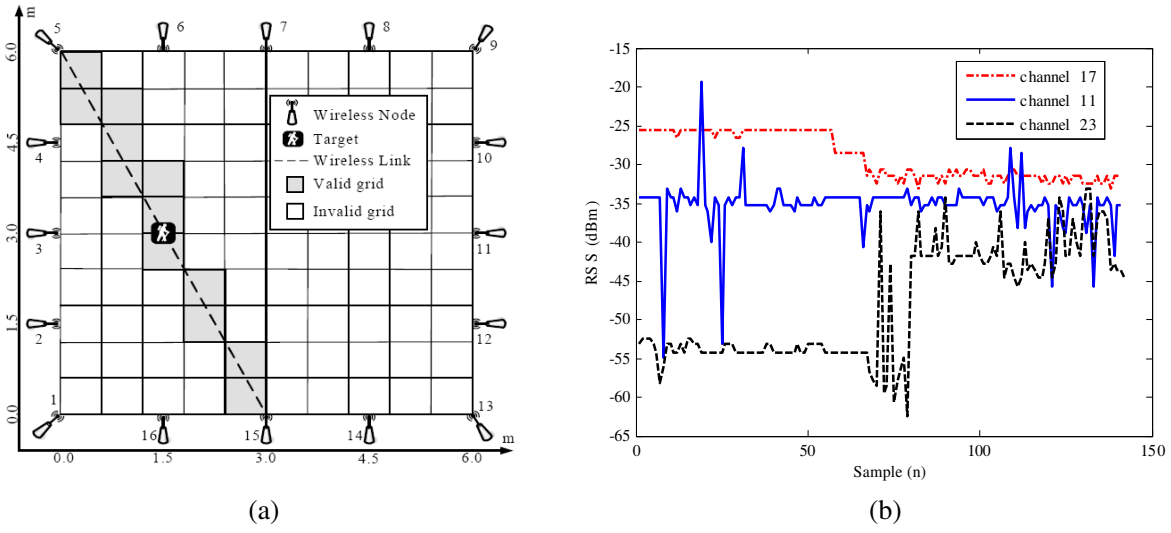

(a) (b)

Figure 1. (a) Illustration of the link measurement. (b) RSS measurements on three different frequency channels.

schemes to select the best channel from the available channels to perform the wireless measurement task. Different from channel selection method in [14], in this paper we adopt the CS-based data fusion approach to combine the data collected on multiple channels. Thus, we can exploit the complementary character of multi-channel RSS measurements to enhance localization performance.

3.2. System Model and Problem Formulation

Consider P unknown-location targets located in an area of interest, which is divided into N square grids. Suppose that Q wireless nodes consist of a wireless network, and each node can work on F independent frequencies. For the SF-DFPL, there will be $M = Q \times (Q-1)/2$ wireless links with every pair of nodes counted as a link, whether or not communication actually occurs between them. However, for the MF-DFPL, there will be $C = M \times F$ virtual wireless links with every pair of nodes working on a specific frequency counted as a link.

So far, the shadowing model is the most widely adopted model to approximate the signal propagation character [8, 15]. With the shadowing model, the measurements $R_t(i, f)$ of link i on the frequency f at time t is described as

$$R_t(i, f) = P_t(i, f) - L_t(i, f) - S_t(i, f) - D_t(i, f) - v_t(i, f) \tag{1}$$

where $P_t(i, f)$ is the transmitted power in dBm, $D_t(i, f)$ the fading loss in decibels, and $L_t(i, f)$ the static losses in decibels due to distance, antenna patterns, device inconsistencies, etc. Generally, these parameters are almost steady and time invariant. $S_t(i, f)$ is the shadowing loss in decibels due to objects that attenuate the signal, and $v_t(i, f)$ is the measurement noise. At time t, the change of the RSS measurement $\Delta R_t(i, f)$ is

$$\Delta R_t(i, f) = R_t(i, f) - R_0(i, f) \approx -S_t(i, f) - v_t(i, f) + v_0(i, f) \tag{2}$$

where $R_0(i, f)$ is the reference RSS measurement that can be learned offline from the link measurements when the deployment area is vacant or that can be learned online with the method proposed in [16]. Generally, measurement noises $v_t(i, f)$ and $v_0(i, f)$ are negligible compared with the shadowing loss. Hence, $\Delta R_t(i, f)$ is primarily determined by the shadowing loss at time t.

Since the deployment area is divided into many grids, the shadowing loss can be approximated as the sum of attenuation that occurs in each square [8–12], hence, $\Delta R_t(i, f)$ can be written as

$$\Delta R_t(i, f) = \sum_{j=1}^{N} w_{ij} x_t(j) + n_t(i, f) \tag{3}$$

where $x_t(j)$ is the difference of attenuation at grid j which corresponds to the fact that whether a target is located in the jth square at time t. $x_t(j)$ will be a significant nonzero value when a target is located at grid j, and in this case, the location of the target is mapped to the value of $x_t(j)$. $n_t(i, f) = -v_t(i, f) + v_0(i, f)$ is the measurement noise, and w_{ij} is the weight that represents the contribution of grid j for link i. According to the past studies, the ellipsoid model with foci at each node location can be used as a method for determining the approximate weight for each link in the network [8, 15]. As a consequence, the weight can be described as

$$w_{ij}(f) = \frac{1}{\sqrt{d_i}} \begin{cases} 1, & \text{if } d_{ij1} + d_{ij2} < d_i + \rho \\ 0, & \text{otherwise} \end{cases} \tag{4}$$

where d_{ij1} and d_{ij2} are the distances from the center of square grid j to the two nodes of link i at frequency f; d_i is the distance between two nodes of link i; ρ represents the width of the ellipse.

When all links in the network are considered simultaneously, the system of RSS measurements can be described in matrix form as

$$\Delta \mathbf{R}_t = \mathbf{W}\mathbf{x}_t + \mathbf{n}_t \tag{5}$$

where $\Delta \mathbf{R}_t$ is a $C \times 1$ vector that is the changes of the RSS measurements; $\mathbf{x}_t = [x_t(1), \ldots, x_t(N)]^T$ is a $N \times 1$ location information vector to be estimated; the $C \times 1$ vector $\mathbf{n}_t$ represents noise terms. $\mathbf{W} = [\mathbf{W}^T(f_1)\ \mathbf{W}^T(f_2) \ldots \mathbf{W}^T(f_F)]^T$ is the $C \times N$ weighting matrix, in which each $M \times N$ matrix $\mathbf{W}(f_k)$, $1 \le k \le F$ represents the weighting matrix at frequency f_k that can be calculated by Eq. (4).

According to the above analysis, the primary objective of the MF-DFPL is to obtain the location vector $\mathbf{x}_t$ from the observations $\mathbf{R}_t$. However, Eq. (5) is usually an ill-posed problem as the condition $C \geq N$ is not always met with a modest set of wireless nodes. Since CS theory is good at solving the underdetermined problem, we will solve this problem with a CS reconstruction algorithm proposed in the following.

4. CS RECONSTRUCTION ALGORITHM WITH PRIOR INFORMATION

Generally, there are a small number of targets or even only one target within the deployment area in DFPL applications. Therefore, the number of targets, P, is considerably smaller than the number of grids N based on sufficient dense gridding, and thus the location information vector $\mathbf{x}_t$ is an extremely sparse signal. Inspired by this fact, references [10–12] attempted to utilize CS theory to tackle the DFPL problem, which leads to

$$\arg\min_{\mathbf{x}_t} \|\mathbf{x}_t\|_1 , \ s.t. \ \Delta\mathbf{R}_t = \mathbf{W}\mathbf{x}_t \tag{6}$$

where $\| \bullet \|_1$ represents the l_1 norm. This problem is an ordinary sparse coding problem and many algorithms have been proposed [17]. However, the recent CS researches reveal that the use of the additional prior information about the sparse representation's support is shown to have advantages in terms of number of required measurements, convergence time and number of iterations [18, 19]. Nonetheless, in DFPL applications this information is not easy to be obtained, since the target to be tracked is generally uncooperative. Moreover, not only are the speed and direction of the target unknown, but also the accurate motion model of the target is unavailable in most cases. The only information about the target available to a DFPL system is its previous location estimate and the assumption that the target's maximum speed is below a threshold $u_{\max}$. To make the algorithm as universal as possible, the prior region $\mathbf{S}_t$ is defined as a circle centered on the previous location estimate

$$\mathbf{S}_t = \{j | H(\mathbf{p}_{t-1}, \mathbf{q}_j) < r, j = 1, \ldots, N\} \tag{7}$$

where $\mathbf{p}_{t-1}$ is the previous location estimate, $\mathbf{q}_j$ the coordinate of a central point of the jth square, $H(\mathbf{p}_{t-1}, \mathbf{q}_j)$ the Euclidean distance between the locations $\mathbf{p}_{t-1}$ and $\mathbf{q}_j$, and r the radius of the circular prior region. The radius r of the prior region is dependent on the maximum distance that the target can travel in the time between sampling instants Δt, i.e., $r \geqslant u_{\max} \times t$. As shown in Fig. 2, the prior region essentially defines the section of the deployment area where the target is most likely to be located next. It must be noted that for $t = 1$, since $\mathbf{p}_0$ is unknown, the radius r is set to a large enough value such that no grids are ignored.

The predicted support set $\mathbf{S}_t$ contains the prior information and indicates which grids the target is more likely located at. When this prior information can be utilized, the sparse recovery problem in

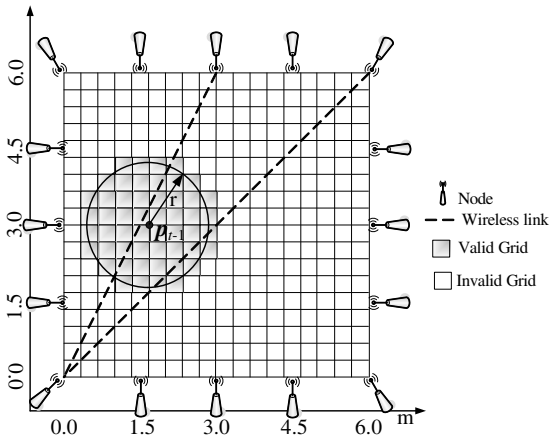

Figure 2. An illustration of the prior region.

Eq. (6) is modified as:

$$\min_{\mathbf{x}_t} \sum_{\substack{k=1 \\ k \notin \mathbf{S}_t}}^{N} |x_t(k)|, \ s.t. \ \Delta\mathbf{R}_t = \mathbf{W}\mathbf{x}_t \tag{8}$$

Note that model in Eq. (8) does not penalize the terms whose indices are in the prior region $\mathbf{S}_t$, which differs from the model in Eq. (6) where all terms are treated. Now, in order to solve Eq. (8), we propose a weighted basis pursuit (WBP) method for sparse signal recovery with prior information. The idea of this method is to introduce weights dependent on the prior information on the positions of nonzero coefficients in the sparse domain into the traditional basis pursuit (BP) algorithm, so that nonzero coefficients in the prior region are favored. Motivated by iteratively reweighted idea in [18, 19], the sparse vector $\mathbf{x}_t$ can then be reconstructed from the measurements $\Delta\mathbf{R}_t$ by solving

$$\min_{\mathbf{x}_t} \sum_{k=1}^{N} \alpha_k^{(m)} |x_t(k)|, \ s.t. \ \Delta\mathbf{R}_t = \mathbf{W}\mathbf{x}_t \tag{9}$$

where $\alpha_k^{(m)}$ is the weighting value to be used in the mth iteration, which is defined

$$\alpha_k^{(m)} = \begin{cases} \left| x_t^{(m-1)}(k) \right|, & \text{if } k \notin \mathbf{S}_t \\ \beta \left| x_t^{(m-1)}(k) \right|, & \text{otherwise} \end{cases} \tag{10}$$

where β is a specified small constant, and $x_t^{(m-1)}(k)$ is the $(m-1)$th iterate in grid k at time t. Note that for $\beta = 0$, the second expression in Eq. (10) reduces to 0. It may be more reasonable to match the definition of the prior region, but $\beta = 0$ may result in divergence in the iterative process. Therefore, a small $\beta > 0$ is necessary for obtaining a feasible solution, and we used $\beta = 0.001$ in our experiments. In summary, the sparse representation $\mathbf{x}_t$ can be reconstructed from measurements $\Delta\mathbf{R}_t$ by solving (9) for $m = 1, 2, \ldots$, until convergence.

5. EXPERIMENTAL RESULTS

5.1. Physical Description of the Experiment

To evaluate the performance of the proposed algorithm, we performed extensive experiments based on a modest wireless network containing 16 nodes in an uncluttered indoor area. A photograph and a map of the experimental setup are shown in Fig. 3. Sixteen wireless nodes are placed 1.5 m apart at the perimeter of a 6 m × 6 m area, and each node is 0.9 m off the ground on a tripod. In addition, a base-station node listens to all broadcasts from the perimeter nodes and logs the RSS information to a mobile computer with 3.1 GHz processor and 4 GB memory for real-time processing.

The transceivers of the nodes are system-on-chip (SoC) CC2530 devices, and each node can work in 16 different frequencies, from 2405 to 2480 MHz with 5 MHz apart. In our experiments, we selected three frequencies (2405, 2435 and 2465 MHz) to realize the MF-DFPL. To avoid network transmission collisions, the whole network is coordinated by the base-station node, and a simple token ring protocol is used to control transmission. Each node is assigned an ID number and programmed with a known order of transmission. After receiving the frequency parameters from the base-station node, the normal nodes begin to perform network scanning. Each node transmits the RSS measurements in turn, and at the same time all the other nodes receive the signal and measure the corresponding RSS values. When one cycle of measurement at one frequency ends, all the nodes in the DFPL system switch to the next frequency under the control of the base-station node. In our tests, it takes 3 ms for each node to broadcast a message, and it takes 48 ms for all the 16 nodes to perform one cycle of measurement. When three frequencies are adopted, the scanning time will be 144 ms.

To obtain the baseline RSS, measurements were taken for 60s while the single human target is outside the deployment area. Afterwards, a target walked inside the deployment area along a predefined trajectory. The default parameters are as follows: grid size is 0.25 m × 0.25 m, the number of grids $N = 576$, width of the ellipse $\rho = 0.3$ m, radius of prior region $r = 1.0$ m and true speed of the target

about 0.5 m/s. The tracking error is defined as the distance between the known true target location and the estimated location obtained by each algorithm. To achieve reliable results, all the statistical results are the average of 50 repeated experiments with independent measurement data for high confidence.

5.2. Performance Analysis and Comparison

The tracking trajectories along the predefined path obtained by the SF-WBP and MF-WBP methods are shown in Fig.? 4, respectively. Although both schemes adopt the WBP algorithm with prior information to realize DFPL estimation, it is shown that the performance of the MF-DFPL is significantly better than the SF-DFPL. Moreover, Fig. 4 also indicates that the tracking errors in the four corners are relatively larger than the others. This phenomenon is mainly due to the fact that when the target changes direction, some transient error will occur while the variations of wireless links traveling through the target are abrupt and discontinuous. Fig. 5 shows the MF-DFPL performance with different numbers of grids N and different widths of the ellipse ρ. We can see that ρ should be a relatively large value to guarantee that the width of the ellipse is wide enough to represent the shadowing effect of the target. As for N, we can see that a larger N will enable the algorithm to achieve better performance. However, the computational complexity of the localization algorithms will increase dramatically with the increase in the number of grids. Hence, N should be a moderate value.

Then, we compare the proposed method with two state-of-the-art CS-based DFPL schemes, i.e., the l_1 norm minimization algorithm in [10] and the greedy-based CMMS algorithm in [11] under the same conditions. Table 1 summarizes detailed statistical results of tracking errors of the SF-DFPL and MF-DFPL with different algorithms. We can find that due to the full utilization of the space-domain prior information of the location vector, the proposed WBP algorithm achieves better performance than the other algorithms. Compared with that of the l_1 and CMMS algorithms in the MF-DFPL, the mean tracking error of the WBP algorithm reduces by 31.8% and 41.4%, respectively. Meanwhile, we can see that although the median values of the tracking errors in three schemes are all less than 0.80 m, the WBP approach has significantly better performance than the other two methods in terms of standard deviation. Moreover, we can see that the performance of the MF-DFPL is better than the traditional SF-DFPL. With the same WBP, l_1 and CMMS algorithms, the mean tracking error of the MF-DFPL reduces by 33.3%, 30.3%, and 27.2%, respectively. The complexity is also compared in terms of the CPU running time from Table 1, which shows that the average running times of the WBP algorithm and l_1 algorithm are almost identical. Although the running time of the WBP method is larger than the CMMS algorithm, this slight growth of complexity is totally acceptable considering the large performance gain that the proposed method achieves.

Furthermore, we evaluate the proposed DFPL scheme under different parameters to analyze its performance. The performance of the proposed scheme with different radius of the circular prior region is shown in Fig. 6. We can see that when r is small, the tracking error is large. As defined by Eq.

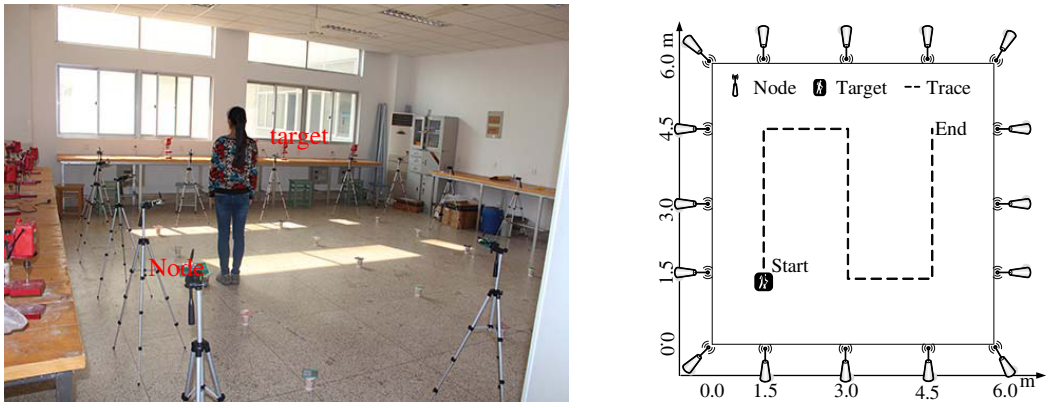

Figure 3. (a) Photograph of the experiment setup. (b) Geometry of the experiment setup.

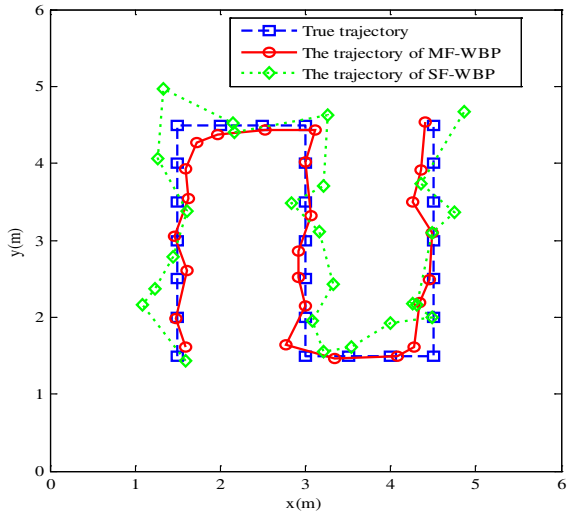

Figure 4. The tracking results along the path.

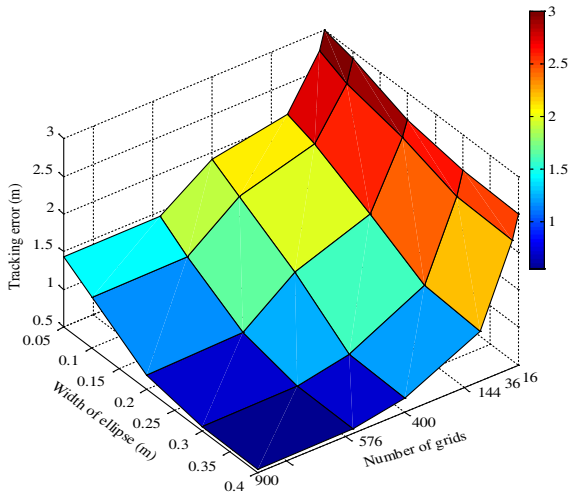

Figure 5. Performance analysis under different numbers of grids N and widths of the ellipse ρ.

Table 1. Comparisons of localization error and average running time.

Algorithm	Average (m)	Median (m)	Standard Deviation (m)	Running Time (ms)
SF-l_1	1.22	0.98	0.82	90.55
SF-CMMS	1.36	1.23	1.01	27.83
SF-WBP	0.87	0.72	0.56	95.67
MF-l_1	0.85	0.69	0.61	191.79
MF-CMMS	0.99	0.80	0.75	75.18
MF-WBP	0.58	0.52	0.33	198.15

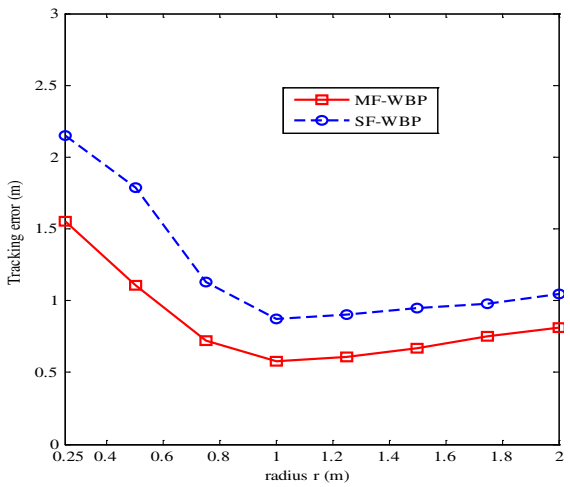

Figure 6. Effects of the different radius of the circular prior region.

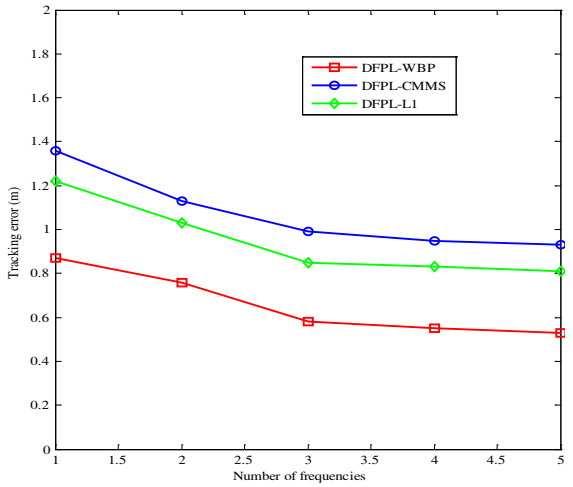

Figure 7. Performance under different numbers of frequencies.

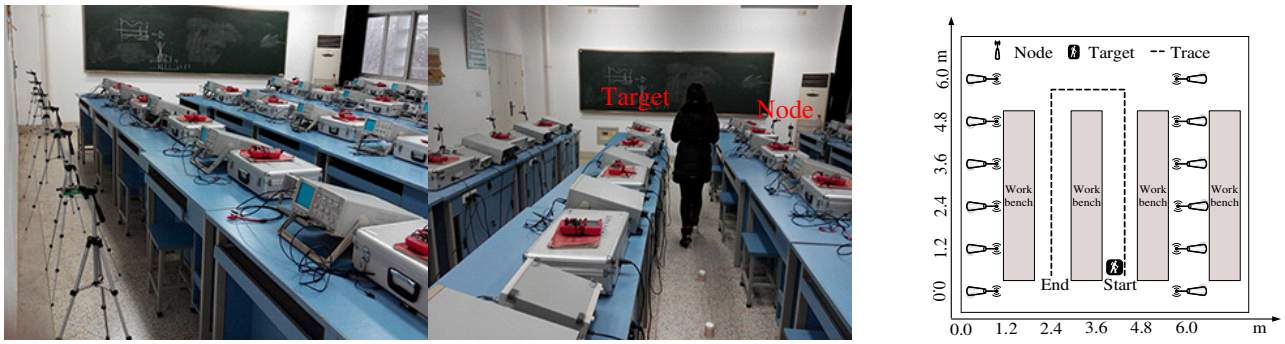

(a) (b)

Figure 8. (a) Photograph of the experiment setup. (b) Geometry of the experiment setup.

(7), the predicted support set $\mathbf{S}_t$ is primarily determined by r. When r is too small, the target will move outside the support set, which leads to misuse of the prior information and then unsatisfactory localization performance. On the other hand, when r is too large, there will be little prior information involved in the prediction operation, and the performance will also drop. Fig. 7 demonstrates the performance with different numbers of frequencies. In addition to the current three frequencies (2405, 2435, and 2465 MHz), we added channel #13 (2415 MHz) and channel #26 (2480 MHz) into MF-DFPL experiments. It is shown that the tracking error reduces gradually with the increase in the number of frequencies, which confirms the effectiveness of the proposed frequency diversity scheme. Meanwhile, we can see that the performance improvement will become less obvious when more frequencies are utilized. This is due to the fact that with the increase in the number of frequencies, the diversity effect will become increasingly inconspicuous.

5.3. Performance in the Heavily Obstructed Indoor Environment

To demonstrate the applicability of the proposed method in rich multipath scenarios, we also carried out an experiment in a highly cluttered indoor environment where many tables and instruments are available. Photos and a map of the experimental setup are shown in Fig. 8. Twelve wireless nodes were deployed to form a 6 m × 6 m area, where nodes were located on two sides of square area. The default parameters are the same as the earlier experiments, except that the nodes are placed 1.2 m apart.

Table 2. Comparisons of localization error and average running time under challenging conditions.

Algorithm	Average (m)	Median (m)	Standard Deviation (m)	Running Time (ms)
SF-l_1	1.37	1.18	0.95	90.76
SF-CMMS	1.62	1.39	1.22	27.80
SF-WBP	0.98	0.85	0.73	96.23
MF-l_1	1.02	0.89	0.77	192.51
MF-CMMS	1.23	1.06	0.93	75.29
MF-WBP	0.76	0.63	0.58	198.55

Table 2 summarizes the detailed statistical tracking results of 50 trials with different algorithms. It is seen from Table 2 that with a modest number of nodes, the SF-WBP algorithm can still track the target with 1 m average accuracy, even in the presence of multiple obstructions in the deployment area. For comparison, the average errors for SF-l_1 and SF-CMMS are 137 m and 1.62 m, respectively. We can also find that the WBP approach has significantly better performance than the other two methods in terms of standard deviation under the complex indoor experiment. Meanwhile, we can see that

the multi-frequency scheme can improve the location estimation performance significantly in the rich multipath environment.

6. CONCLUSION

To achieve satisfactory localization and tracking results in the indoor environment using the modest set of wireless nodes, a novel DFPL scheme which utilizes the multiple channels information has been proposed. Inspired by the thought of diversity widely adopted in wireless communications and the fact that the influence of the noise for different channels is also different, we combined the frequency diversity technique and CS theory into a unified DFPL framework. This method can not only take advantage of CS to handle the inherent spatial sparsity of the DFPL problem in the spatial domain, but also make use of link information of multi-channel simultaneously to reduce the impact of the RSS sensitivity. Furthermore, based on the fact that the location information of the target is not only sparse but also changes continuously over time, we proposed a particular CS reconstruction method by utilizing the prior information on the support region obtained from last target's location estimation to improve sparse reconstruction performance. The effectiveness of the proposed scheme has been demonstrated by experimental results where substantial improvement for localization performance is achieved with a few nodes. Future work will emphasize the theoretic bound on the location estimation precision and extend the proposed algorithm for use in multi-target tracking.

ACKNOWLEDGMENT

This work was supported by the Specialized Research Fund for the Doctoral Program of Higher Education of China (Grant No. 20133207120007), and the Open Research Fund of Jiangsu Key Laboratory of Meteorological Observation and Information Processing (Grant No. KDXS1408).

REFERENCES

1. Mitilineos, S. A. and S. C. A. Thomopoulos, "Positioning accuracy enhancement using error modeling via a polynomial approximation approach," *Progress In Electromagnetics Research*, Vol. 102, 49–64, 2010.
2. Mitilineos, S. A., D. M. Kyriazanos, O. E. Segou, J. N. Goufas, and S. C. A. Thomopoulos, "Indoor localization with wireless sensor networks," *Progress In Electromagnetics Research*, Vol. 109, 441–474, 2010.
3. Patwari, N. and J. Wilson, "RF sensor networks for device-free localization: Measurements, models, and algorithms," *Proc. of the IEEE*, Vol. 98, No. 11, 1961–1973, 2010.
4. Youssef, M., M. Mah, and A. Agrawala, "Challenges: Device-free passive localization for wireless environments," *13th ACM MobiCom.*, 222–229, 2007.
5. Sabek, I., M. Youssef, and A. V. Vasilakos, "ACE: An accurate and efficient multi-entity device-free WLAN localization system," *IEEE Transactions on Mobile Computing*, Vol. 14, No. 2, 261–273, 2015.
6. Zhang, D., J. Ma, Q. Chen, and L. M. Ni, "An RF-based system for tracking transceiver-free objects," *Proc. 5th PerCom.*, 135–144, 2007.
7. Zhang, D., K. Lu, R. Mao, Y. Feng, Y. Liu, Z. Ming, and L. Ni, "Fine-grained localization for multiple transceiver-free objects by using RF-based technologies," *IEEE Trans. Parallel Distrib. Syst.*, Vol. 25, No. 6, 1464–1475, 2014.
8. Wilson, J. and N. Patwari, "Radio tomographic imaging with wireless networks," *IEEE Transactions on Mobile Computing*, Vol. 9, No. 5, 621–632, 2010.
9. Kaltiokallio, O., M. Bocca, and N. Patwari, "A fade level-based spatial model for radio tomographic imaging," *IEEE Transactions on Mobile Computing*, Vol. 13, Vo. 5, 1159–1172, 2014.
10. Kanso, M. A. and M. G. Rabbat, "Compressed RF tomography for wireless sensor networks: Centralized and decentralized approaches," *Proc. 5th DCOSS*, 173–186, 2009.

11. Yang, Z. Y., K. D. Huang, X. M. Guo, and G. L. Wang, "A real-time device-free localization system using correlated RSS measurements," *EURASIP J. Wireless Commu. Netw.*, Vol. 2013, No. 186, 1–12, 2013.
12. Wang, J., Q. Gao, X. Zhang, and H. Wang, "Device-free localization with wireless networks based on compressing sensing," *IET Commun.*, Vol. 6, No. 15, 2395–2403, 2012.
13. Ke, W., G. Liu, and T. Fu, "Robust sparsity-based device-free passive localization in wireless networks," *Progress In Electromagnetics Research C*, Vol. 46, 63–73, 2014.
14. Kaltiokallio O., M. Bocca, and N. Patwari, "Enhancing the accuracy of radio tomographic imaging using channel diversity," *Proc. 9th IEEE Int. Conf. MASS*, 254–262 2012.
15. Hamilton B. R., X. L. Ma, R. J. Baxley, and S. M. Matechik, "Propagation modeling for radio frequency tomography in wireless networks," *IEEE J. Sel. Topics Signal Process*, Vol. 8, No. 1, 43–54, 2014.
16. Zhao Y. and N. Patwari, "Demo abstract: Histogram distance-based radio tomographic localization," *Proc. 11th ACM/IEEE Int. Conf. IPSN*, 129–130, 2012.
17. Candès, E. J. and M. B. Waki, "An introduction to compressive sampling," *IEEE Signal Process. Mag.*, Vol. 25, No. 2, 21–30, 2008.
18. Miosso C. J., R. Von Borries, and J. H. Pierluissi, "Compressive sensing with prior information: Requirements and probabilities for reconstruction in l_1-minimization," *IEEE Trans Signal Process.*, Vol. 61, No. 9, 2150–2164, 2013.
19. Scarlett, J., J. S. Evans, and S. Dey, "Compressed sensing with prior information: information-theoretic limits and practical decoders," *IEEE Trans. Signal Process.*, Vol. 61, No. 2, 427–439, 2013.